Tailorable three-dimensional distribution of laser foci based on customized fractal zone plates

2013 Laser Phys. Lett. 10 035003

(http://iopscience.iop.org/1612-202X/10/3/035003)

IOP PUBLISHING LASER PHYSICS LETTERS
Laser Phys. Lett. **10** (2013) 035003 (6pp) doi:10.1088/1612-2011/10/3/035003

LETTER

Tailorable three-dimensional distribution of laser foci based on customized fractal zone plates

S H Tao[1], B C Yang[1], H Xia[2] and W X Yu[3]

[1] Institute of Super Microstructure and Ultrafast Process, School of Physics and Electronics, Central South University, Changsha, Hunan 410083, People's Republic of China
[2] School of Physics and Electronics, Central South University, Changsha, Hunan 410083, People's Republic of China
[3] State Key Laboratory of Applied Optics, Changchun Institute of Optics, Fine Mechanics and Physics, Chinese Academy of Sciences, Changchun, Jilin 130033, People's Republic of China

E-mail: eshtao@csu.edu.cn and yuwx@ciomp.ac.cn

Received 18 July 2012, in final form 11 November 2012
Accepted for publication 15 November 2012
Published 5 February 2013
Online at stacks.iop.org/LPL/10/035003

Abstract
There is high demand for a tailorable three-dimensional (3D) distribution of focused laser beams for simultaneous optical manipulation of multiple particles separately distributed in 3D space. In this letter, accurate control of the 3D distribution of laser beam foci is demonstrated with an array of customized fractal zone plates (FZPs). The FZPs are designed with a fractional number of fractal segments, so the focal lengths of the foci can be finely tailored. The unique focusing properties of the customized FZPs are investigated with both simulations and experiments. The FZP beams are also found to possess the self-reconstruction property, which would be useful for constructing 3D optical tweezers.

(Some figures may appear in colour only in the online journal)

1. Introduction

In optical trapping, highly focused laser beams are widely used to invasively trap micro- and even nano-particles, located around the focus of a beam. Since conventional optical beams have controllable optical fields in the imaging planes only, multiple particles in different planes cannot be manipulated simultaneously. Although a hologram that is designed by phase retrieval algorithms can reconstruct different images in multiple imaging planes, a distortion made by reflection, refraction, or absorption of a trapped particle would affect the subsequent propagation of the beam. To trap multiple particles separately distributed in three-dimensional (3D) space, we have to generate a beam which has not only tailorable 3D intensity distribution, but also the self-reconstruction property [1]. Only a few optical beams, such as Bessel beams and families of propagation-invariant optical beams, Airy beams, and others [2–6], have been found to have the self-reconstruction property. The Bessel beams were used to manipulate multiple particles simultaneously [2], but positions of trapped particles in 3D space could not be customized owing to the nature of the non-diffracting property of the beams. Fractal zone plates (FZPs) [7] have unique diffraction properties [8–10] and potential applications in the fields of optical trapping and beam shaping. Apart from the main focus, many weaker foci, namely major foci, also appear along the optical axis of an FZP beam. As focal lengths of multiple foci provided by an FZP are determined by the structural parameters of the FZP, the axial distances between the neighboring foci of the beam can be designed

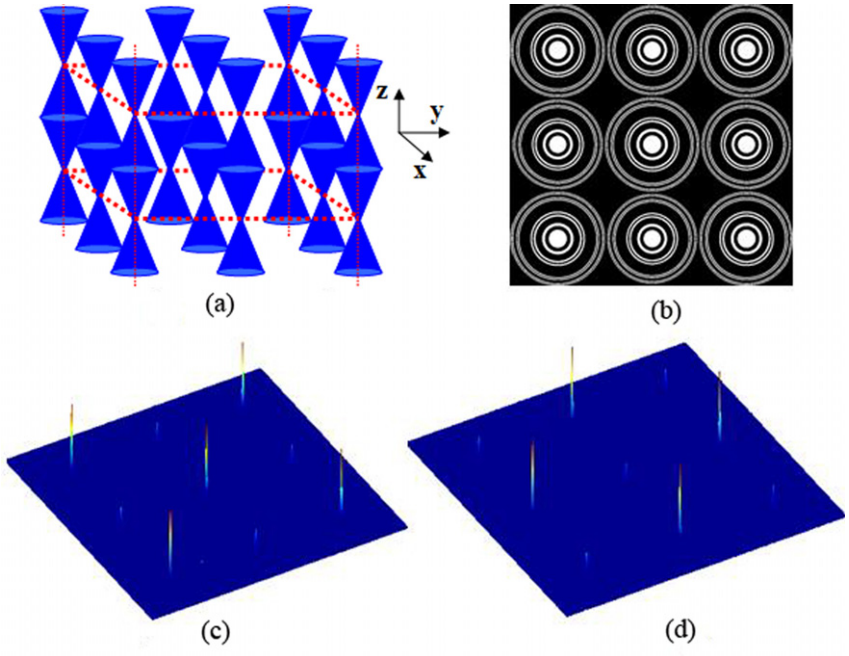

Figure 1. (a) An example of an array of 3 × 3 FZP beams forming cubic-like structure and (b) phase distribution of an array of 3 × 3 FZPs with slightly varying pupil size; (c) and (d) the intensity distributions in the main focal planes of the FZPs with $a = 1.15$ mm and $a = 1.09$ mm, respectively.

beforehand. Although many customized FZPs [11–18] have been proposed, the number of fractal segments of an FZP has always been taken as an integer. Thus, the axial distance between two neighboring foci of an FZP beam can only be roughly adjusted, and the positions of multiple particles trapped by the beam would not be precisely controlled. In this letter we propose a method of generation of an array of FZP beams with a single phase plate, which comprises an array of customized FZPs. In the array, the number of segments forming the fractal structure of an FZP can be fractional and the structure of each FZP can be tailored, thus light diffraction distributions both in imaging planes and axial positions can be precisely controlled. Furthermore, the FZP beams are found to have the self-reconstruction property. With the unique diffraction properties, the FZP beam can be employed to construct 3D optical tweezers, which simultaneously trap multiple particles distributed separately in 3D space.

2. Design and simulation

An expression for the transmittances of a single FZP can be found in [7], where the values are always 0 or 1, meaning that they are opaque or transparent to the incident beam. The focal length of the main focus of an FZP beam can be expressed by equation (1) [7–9]

$$f(a, \lambda, N, S) = a^2 \cdot [\lambda \cdot (2N - 1)^S]^{-1}, \qquad (1)$$

where a is the radius of the FZP, λ the wavelength of the illuminating light, N the number of segments forming the fractal structure, and S the fractal stage. Major foci of the beam are positioned symmetrically around the main focus in the axial direction under the normalized dimensionless axial coordinate $u = a^2 \cdot (2\lambda z)^{-1}$ [7–9]. As the wavelength of a laser beam in beam shaping is usually constant, λ will not be considered as a variable in our design. S can only be an integer, and N has been regarded as an integer in the literature. However, if N changes with the smallest step of 1, the resultant focal length will still vary significantly. Hence, to finely tune the focal length of an FZP beam, we will treat N as a fraction.

As phase-only diffractive optical elements have higher diffraction efficiency than the amplitude-only counterparts, the transmittance values of 0 and 1 of the FZP will be replaced with phase steps of 0 and π, respectively [11]. Figure 1(a) illustrates schematically a cubic-like structure realized by an array of 3 × 3 FZP beams. The phase distribution of an array of 3 × 3 FZPs with slightly varying pupil size is shown in figure 1(b), where black and white represent phase 0 and π, respectively. The parameters of the FZPs in figure 1(b) are $S = 3$, $N = 2$, and $\lambda = 532$ nm. a is set as 1.15 mm for the FZPs in the corners and center of the figure, and 1.09 mm for the FZPs in the other positions. Thus, the resultant axial distance difference between the main foci of the two FZP beams is less than 1 mm. Propagations of the FZP beams in free space are simulated by using the angular spectrum of the plane wave method. 3D irradiances at the main focal length, 9.2 mm, for the FZPs with $a = 1.15$ mm are present in figure 1(c), and irradiances at the main focal length, 8.3 mm, for the FZPs with $a = 1.09$ mm are shown in figure 1(d). It can be seen that laser beam foci can be made to appear at alternating positions of the two focal planes.

Figure 2(a) shows an array of 3 × 3 FZPs with fractional N, which increases from 2.0 to 2.8 with an increment of 0.1. Pupils of all the FZPs have the same size. The FZPs

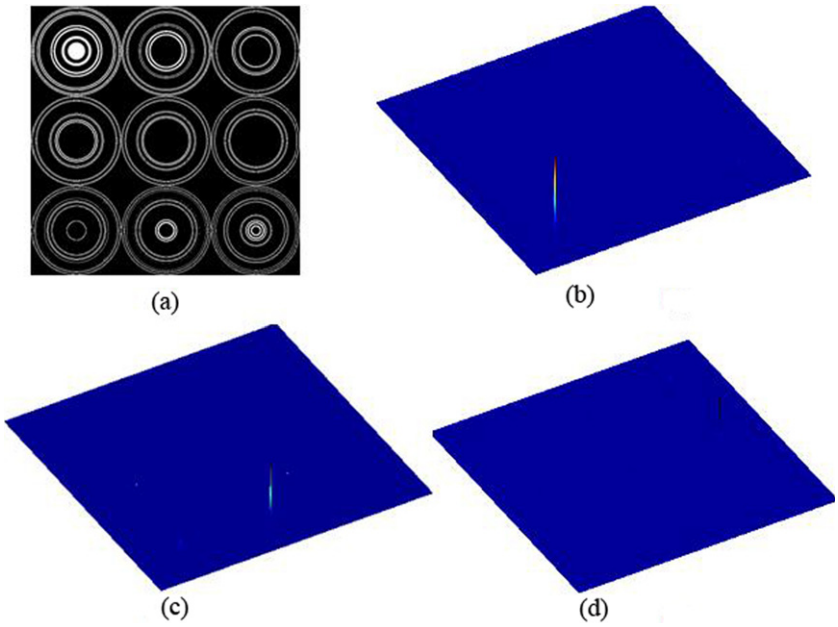

Figure 2. (a) Phase distribution of 3 × 3 FZPs with varying N; (b)–(d) the intensity distributions in the focal planes of the FZPs with $N = 2.0$, $N = 2.1$, and $N = 2.5$, respectively.

with $N = 2.0$, 2.1, and 2.2 are arranged from left to right in the top row, and the remaining FZPs are arranged in the array in a similar way. Irradiances at the focal planes of the FZP beams with $N = 2.0$, $N = 2.1$, and $N = 2.5$ are shown in figures 2(b)–(d), respectively. It is worth mentioning that the FZPs in figure 2(a) and the reconstructed beams in figures 2(b)–(d) are not shown in the same orientation. With simulations we have verified that the focal length of an FZP beam with fractional N can still be expressed by equation (1). However, we can observe that an FZP beam with fractional N has weaker foci than the FZP beams with an integer of N. In the range of N from 2.0 to 3.0, the intensity magnitude of the main focus of an FZP beam with varying N is found to fluctuate with the area ratio, which is defined as the ratio between the areas of the bright and dark regions of an FZP. The area ratio of an FZP varies in a parabolic way with the increase of N. As the FZP with $N = 2.5$ has the lowest area ratio whereas the FZP with $N = 2.0$ has the highest area ratio that is closest to 1, the main focus of the FZP beam with $N = 2.5$ has the lowest intensity and that of the FZP beam with $N = 2.0$ has the highest intensity.

As an FZP comprises many narrow rings, each of which will generate a Bessel beam during the light propagation, the rings of different radii will generate a superposition of Bessel beams with different radial components of the wave vector. The superposition of interfering Bessel beams has been proven to be self-reconstructive [3]. Thus, the FZP beam would possess the self-reconstruction property, too. We will use simulations to verify the property of the FZP beams. In the light propagation, an opaque object with a radius of 38.4 μm is placed in the center of the beam at a propagating distance of 73.8 mm, where a major focus of the FZP beam is located. The opaque object blocks light passing through the center of the major focus at a distance of 73.8 mm. The parameters of the FZP are $N = 2$, $S = 3$, and $a = 1.15$ mm. Intensity profiles of the obstructed and unobstructed beams are shown in figures 3(a) and (d) at propagating distances of $z = 78.4$ mm, (b) and (e) at $z = 87.6$ mm, and (c) and (f) at $z = 143$ mm, respectively. It can be seen from figure 3 that although the central part of the major focus is totally blocked by the opaque object, the obstructed beam still recovers in several millimeters. The beams shown in figures 3(c) and (f) look nearly identical, demonstrating that the obstructed beam is self-reconstructive.

For a further comparison between the light propagations, cross-sections of the obstructed and unobstructed beams were sampled with a step of 4.6 mm along the axial direction and are presented in figure 4, where (a) and (b) represent the obstructed and unobstructed beams in the propagation, respectively. For a better view, only the central parts of the beams are displayed in figure 4, where the vertical size of the beam is 0.64 mm in diameter, and the horizontal axis represents a propagating distance which ranges from 46 to 184 mm. A total of 30 intensity cross-sections were sampled.

The opaque object is placed in the center of the sixth intensity cross-section in figure 4(a). We can observe that both the obstructed and unobstructed beams are nearly identical after a short propagating distance. Hence, the FZP beam possesses the self-reconstruction property. Furthermore, with the simulations we find that the FZP beams with fractional N also possesses the self-reconstruction property. The generation of arrays of the FZP beams can also be customized with the introduction of spiral phases or a composition of other forms of FZPs [11, 17]. Thus, the freedom to achieve the desired 3D distribution of laser foci would be further enhanced.

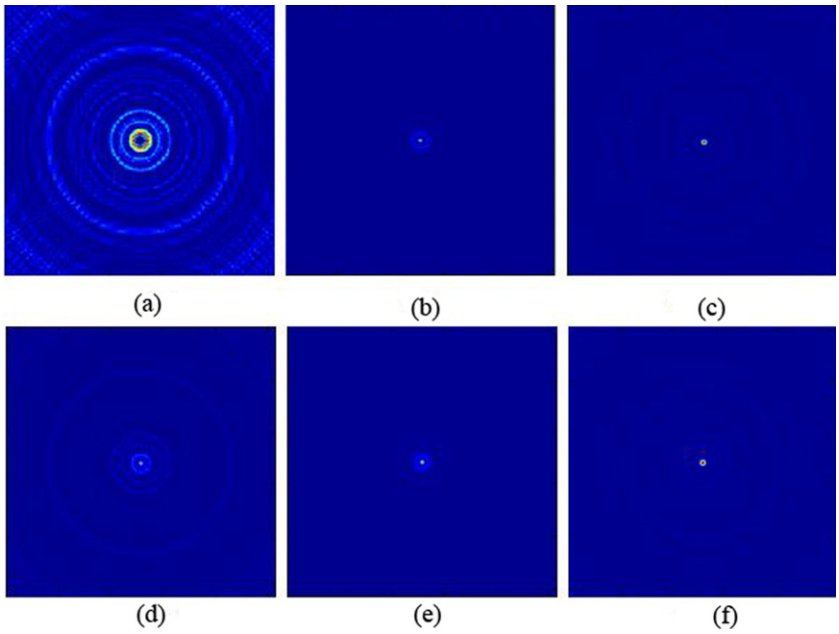

Figure 3. Intensity distributions of the obstructed beam at propagating distances of (a) $z = 78.4$ mm, (b) $z = 87.6$ mm, and (c) $z = 143$ mm, respectively. Intensity distributions of the unobstructed beam at propagating distances of (d) $z = 78.4$ mm, (e) $z = 87.6$ mm, and (f) $z = 143$ mm, respectively.

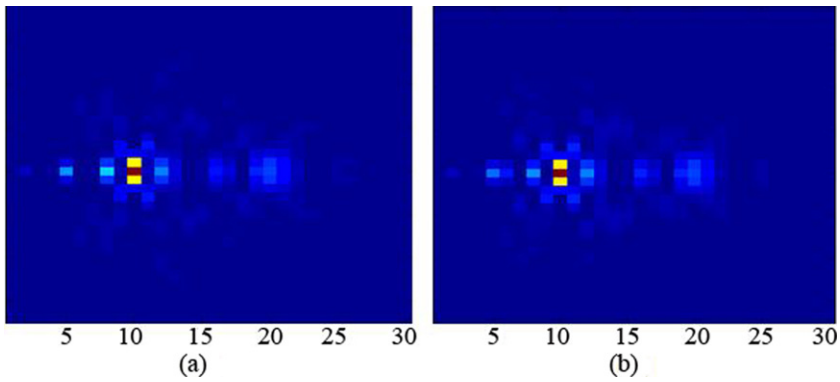

Figure 4. Sampled intensity distributions of (a) the obstructed beam and (b) the unobstructed beam versus the propagating distances. In (a) the obstacle is placed in the center of the sixth sampled intensity cross-section.

3. Experiment

In the experiments, a 532 nm solid-state laser is used. Firstly, the laser beam is expanded and collimated by a spatial filter and a convex lens. Then the laser beam passes through a polarization cube. A linearly polarized beam refracted from the cube is incident on a spatial light modulator (SLM) and reflected. The SLM comprises 1024 × 768 pixels, and the pixel pitch is 9 μm. Finally, intensities of the reflected beam from the SLM at different propagating distances are captured by a CCD beam profiler. The gray-scale image shown in figure 1(b) is loaded onto the SLM. The loaded image comprises 3 × 3 FZPs with varying pupil size and each FZP has 256 × 256 pixels. Figures 5(a)–(f) present the recorded intensity profiles at estimated propagating distances of 14 cm, 18 cm, 24 cm, 26 cm, 28 cm, and 31 cm, respectively. Thus, laser foci appearing at the desired lateral and axial positions have been realized with the customized FZPs.

Then the array of FZPs with fractional N, shown in figure 2(a), is loaded onto the SLM screen. The captured intensity profiles of the reflected beam at estimated propagating distances of 12 cm, 19 cm, and 21 cm are shown in figures 6(a)–(c), respectively. It can be seen that the beams are focused in turn at different positions in the array with varying propagating distances. The brightest spots in the figures appear at the positions of the FZPs with (a) $N = 2.0$, (b) $N = 2.5$, and (c) $N = 2.1$, respectively. It can also be observed that the intensities of the focused spots with fractional N are weaker than those with $N =$

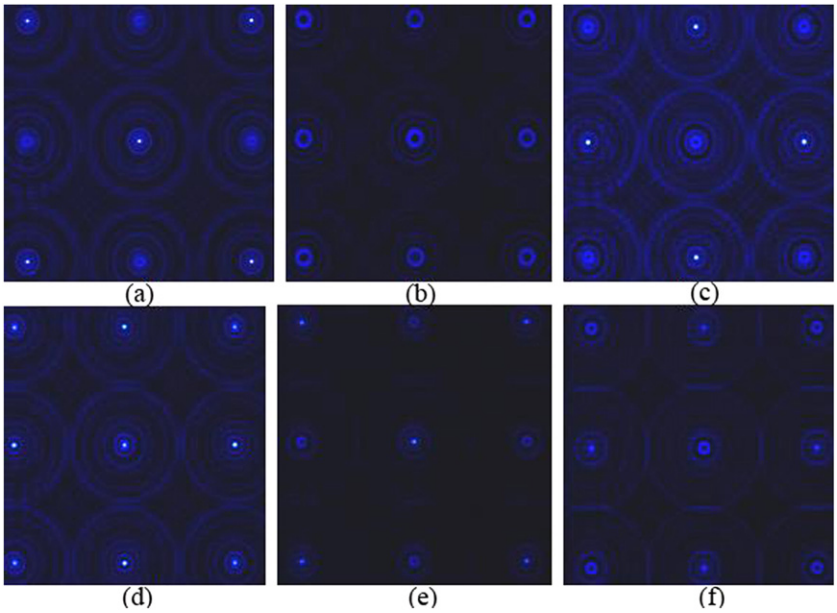

Figure 5. (a)–(f) show the captured intensity distributions diffracted by the FZPs in figure 1(b). The propagating distances for (a)–(f) are about 14 cm, 18 cm, 24 cm, 26 cm, 28 cm, and 31 cm, respectively.

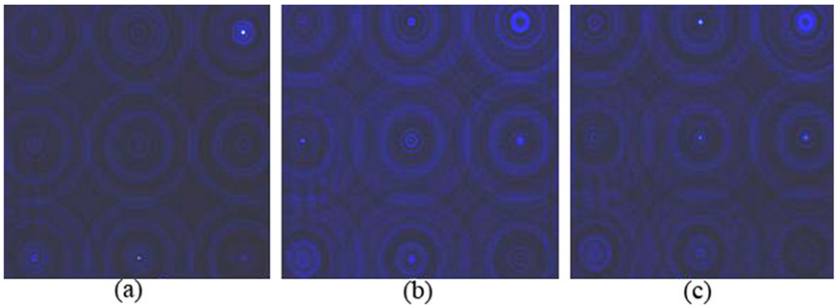

Figure 6. Captured intensity profiles diffracted by the FZPs in figure 2(a). The brightest spots appear at the positions of the FZPs with (a) $N = 2.0$, (b) $N = 2.5$, and (c) $N = 2.1$, respectively, and the propagating distances are about 15 cm, 19 cm, 21 cm, respectively.

2.0. The experimental results are compatible with the simulations.

4. Conclusion

To summarize, we have used an array of FZPs with adjustable structural parameters to generate a 3D distribution of laser beam foci. The FZPs are designed with fractional structural parameters and a customized arrangement of positions of the FZPs in an array. Various 3D distributions of multiple foci have been demonstrated both in simulations and experiments. The FZP beam has also been found to possess the self-reconstruction property. The unique diffraction properties of the FZP beams would be useful for constructing 3D optical tweezers.

Acknowledgments

The research was financially supported by the Natural Science Foundation of Hunan Province, China (grant no. 11JJ22039) and the National Natural Science Foundation of China (grant nos 61178017 and 61172047).

References

[1] Bouchal Z, Wagner J and Chlup M 1998 *Opt. Commun.* **151** 207
[2] Garcés-Chávez V, McGloin D, Melville H, Sibbett W and Dholakia K 2002 *Nature* **419** 145
[3] McGloin D, Garcés-Chávez V and Dholakia K 2003 *Opt. Lett.* **28** 657
[4] Tao S H and Yuan X C 2004 *J. Opt. Soc. Am.* A **21** 1192
[5] Broky J, Siviloglou G A, Dogariu A and Christodoulides D N 2008 *Opt. Express* **16** 12880
[6] Anguiano-Morales M, Martínez A, David Iturbe-Castillo M, Chávez-Cerda S and Alcalá-Ochoa N 2007 *Appl. Opt.* **46** 8284
[7] Saavedra G, Furlan W D and Monsoriu J A 2003 *Opt. Lett.* **28** 971
[8] Monsoriu J A, Saavedra G and Furlan W D 2004 *Opt. Express* **12** 4227
[9] Davis J A, Ramirez L, Rodrigo Martín Romo J A, Alieva T and Calvo M L 2004 *Opt. Lett.* **2** 1321

[10] Dai H, Liu J, Sun X and Yin D 2008 *Opt. Commun.* **281** 5515
[11] Tao S H, Yuan X-C, Lin J and Burge R 2006 *Appl. Phys. Lett.* **89** 031105
[12] Furlan W D, Saavedra G and Monsoriu J A 2007 *Opt. Lett.* **32** 2109
[13] Monsoriu J A, Furlan W D, Saavedra G and Giménez F 2007 *Opt. Express* **15** 13858
[14] Wu D, Niu L-G, Chen Q-D, Wang R and Sun H-B 2008 *Opt. Lett.* **33** 2913
[15] Calatayud A, Monsoriu J A, Mendoza-Yero O and Furlan W D 2009 *J. Opt. Soc. Am.* A **26** 2532
[16] Mendoza-Yero O, Fernández-Alonso M, Mínguez-Vega G, Lancis J, Climent V and Monsoriu J A 2009 *J. Opt. Soc. Am.* A **26** 1161
[17] Furlan W D, Giménez F, Calatayud A and Monsoriu J A 2009 *Opt. Express* **17** 21891
[18] Giménez F, Furlan W D, Calatayud A and Monsoriu J A 2010 *J. Opt. Soc. Am.* A **27** 1851